



A Segmented Period–Luminosity Relation for Nearby Extragalactic Delta Scuti Stars

C. E. Martínez-Vázquez^{1,2} , R. Salinas³ , A. K. Vivas² , and M. Catelan^{4,5} ¹ Gemini Observatory/NSF's NOIRLab, 670 N. A'ohoku Place, Hilo, HI 96720, USA; clara.martinez@noirlab.edu² Cerro Tololo Inter-American Observatory/NSF's NOIRLab, Casilla 603, La Serena, Chile³ Gemini Observatory/NSF's NOIRLab, Casilla 603, La Serena, Chile⁴ Pontificia Universidad Católica de Chile, Facultad de Física, Instituto de Astrofísica, Av. Vicuña Mackenna 4860, 782-0436 Macul, Santiago, Chile⁵ Millennium Institute of Astrophysics, Santiago, Chile

Received 2022 October 14; revised 2022 November 2; accepted 2022 November 2; published 2022 November 22

Abstract

The period–luminosity relations (PLRs) of Milky Way δ Scuti (δ Sct) stars have been described to the present day by a linear relation. However, when studying extragalactic systems such as the Magellanic Clouds and several dwarf galaxies, we notice for the first time a nonlinear behavior in the PLR of δ Sct stars. Using the largest sample of ~ 3700 extragalactic δ Sct stars from data available in the literature—mainly based on the Optical Gravitational Lensing Experiment and the Super MAssive Compact Halo Object project in the Large Magellanic Cloud (LMC)—we obtain that the best fit to the period–luminosity (M_V) plane is given by the following piecewise linear relation with a break at $\log P = -1.03 \pm 0.01$ (or 0.093 ± 0.002 days) for shorter periods (sp) and longer periods (lp) than the break-point:

$$M_V^{\text{sp}} = -7.08(\pm 0.25)\log P - 5.74(\pm 0.29); \quad \log P < -1.03$$

$$M_V^{\text{lp}} = M_V^{\text{sp}} + 4.38(\pm 0.32) \cdot (\log P + 1.03(\pm 0.01)); \quad \log P \geq -1.03.$$

Geometric or depth effects in the LMC, metallicity dependence, or different pulsation modes are discarded as possible causes of this segmented PLR seen in extragalactic δ Sct stars. The origin of the segmented relation at ~ 0.09 days remains unexplained based on the current data.

Unified Astronomy Thesaurus concepts: [Delta Scuti variable stars \(370\)](#); [SX Phoenicis variable stars \(1673\)](#); [Variable stars \(1761\)](#); [Dwarf galaxies \(416\)](#); [Globular star clusters \(656\)](#)

1. Introduction

The period–luminosity relations (PLRs) of pulsating variable stars are undoubtedly one of the cornerstones of modern astrophysics. In particular, the PLR for classical Cepheids (Leavitt & Pickering 1912) permitted establishing the nature of *nebulae* as galaxies (Hubble 1925), the discovery of the expansion of the universe (Hubble 1929), and the first rung in the distance scale, and the existence of dark energy (e.g., Riess et al. 2019). Not as tight as the PLR for Cepheids in the visible, but uniquely tracing old (≥ 10 Gyr) populations, the PLR of RR Lyrae stars (e.g., Catelan et al. 2004) has also provided precise distances to, for example, the Galactic center (Dekany et al. 2013), globular clusters (Braga et al. 2015; Neeley et al. 2015; Braga et al. 2018), and dwarf galaxies in the Local Group (e.g., Martínez-Vázquez et al. 2015; Vivas et al. 2016; Martínez-Vázquez et al. 2017, 2019; Vivas et al. 2022).

Being fainter and with shorter periods (0.008–0.42 days) and lower amplitudes (0.001–1.7 mag in V) than Cepheids and RR Lyrae (e.g., Catelan & Smith 2015), δ Scuti stars (hereafter δ Sct), in the intersection of the main sequence and the instability strip, are standard candles that follow not very popular PLRs. Despite their lower brightness, their value comes from tracing young, and especially *intermediate* age populations, partly filling the age gap between Cepheids and RR Lyrae stars. They can also be more numerous than RR Lyrae stars (e.g., Vivas & Mateo 2013).

As intrinsically fainter stars, precise distances are more difficult to obtain, but also the construction of their PLRs requires the determination of their pulsation mode, and to understand the effect of the metallicity and evolutionary stage. Despite these difficulties, many PLRs have been explored, both theoretically and empirically (e.g., Nemeč et al. 1994; McNamara 2011; Fiorentino et al. 2015; Ziaali et al. 2019; Jayasinghe et al. 2020; Barac et al. 2022). Of particular interest is the work of Cohen & Sarajedini (2012), connecting both δ Sct and SX Phe stars, their metal-poor counterparts, into a single PLR, suggesting largely an independence of metallicity effects.

In this Letter, we revisit the δ Sct PLRs given in the literature and derive a new PLR for nearby extragalactic δ Sct stars.

2. Data

We have gathered data available in the literature associated with δ Sct and SX Phe studies to perform a comprehensive analysis of their PLRs. To do that, we have used several catalogs that report periods and mean magnitudes (particularly in the V band) for the δ Sct and SX Phe stars (collectively also known as dwarf Cepheids; see Mateo et al. 1993; Vivas & Mateo 2013).

For the Large Magellanic Cloud (LMC) we have used the δ Sct stars catalogs of the Optical Gravitational Lensing Experiment-III (OGLE-III; Poleski et al. 2010) and the Super Massive Compact Halo Object (SuperMACHO) project (Garg et al. 2010). Additionally, we have included the δ Sct from the LMC cluster NGC 1846 and its surrounding field (Salinas et al. 2018). For the Small Magellanic Cloud (SMC), we have used OGLE-II (Soszynski et al. 2002) and the recent work of Martínez-Vázquez et al. (2021) in the SMC cluster NGC 419.

Table 1
Distance Moduli, Extinctions, and Metallicities

System	$\mu_0^{(a)}$	A_V	$\langle[\text{Fe}/\text{H}]\rangle^{(b)}$
LMC ^(c)	18.476	0.40	-0.5
NGC 1846	18.45	0.09	-0.5
SMC	18.97	0.28	-1.0
NGC 419	18.85	0.15	-0.55
Carina	20.01	0.09	-1.0
Fornax	20.72	0.06	-1.7
Sculptor	19.62	0.06	-1.7
Sextans	19.64	0.14	-1.9
GGCs	:	:	$[-2.35, -0.59]$
Galactic field	^(d)	^(d)	$[-0.5, 0.3]$

Note. (a) References for distances and average extinction: LMC (Westerlund 1997; Pietrzynski et al. 2019); NGC 1846 (Goudfrooij et al. 2009); SMC (Westerlund 1997; Graczyk et al. 2014); NGC 419 (Goudfrooij et al. 2014); Carina (Coppola et al. 2015); Fornax (Rizzi et al. 2007); Sculptor (Martínez-Vázquez et al. 2016); Sextans (Vivas et al. 2019); Galactic globular clusters (GGCs; Harris 1996; Baumgardt & Hilker 2018, 2010 edition). (b) References for mean metallicities: LMC and NGC 1846 (Grocholski et al. 2006; Carrera et al. 2008b); SMC and NGC 419 (Carrera et al. 2008a; Mucciarelli 2014, A. Mucciarelli 2020, private communication); Sextans (Kirby et al. 2011); Carina (Koch et al. 2006); Fornax and Sculptor (Kirby et al. 2013); GGCs (Carretta et al. 2009); Galactic Field (Jayasinghe et al. 2020). (c) For the LMC we use individual instead of the mean distance and absorption values. See Section 3.1 for more details. (d) For the Galactic field we used the M_V values provided by Ziaali et al. (2019); thus μ_0 and A_V were not required.

For the δ Sct/SX Phe stars in dwarf galaxies in the Local Group we have collected the data from the following works: Fornax (Poretti et al. 2008), Carina (Vivas & Mateo 2013; Coppola et al. 2015), Sculptor (Martínez-Vázquez et al. 2016), and Sextans (Vivas et al. 2019).

As a comparison to the extragalactic sample, we have used different Galactic δ Sct studies. To start, we have employed the Ziaali et al. (2019) catalog, which is a compilation of the Rodríguez et al. (2000) catalog, and in addition, δ Sct stars studied with Kepler (Murphy et al. 2019), with distances from Gaia DR2 (Gaia Collaboration et al. 2018). Finally, for the Galactic globular clusters we have employed the compilation made by Cohen & Sarajedini (2012).

Table 1 lists the most updated distance moduli available in the literature and mean extinctions used in this work for each of these systems.

3. Period–Luminosity Relation of δ Sct Stars

In the following, we will show how a break in the PLR of extragalactic δ Sct stars arises from literature data, and how it is largely independent on the assumptions used for distance, reddening, and metallicity effects.

3.1. LMC

The OGLE and SuperMACHO survey discovered more than ~ 4500 δ Sct stars in the LMC (Poleski et al. 2010; Garg et al. 2010, respectively). However, due to the different goals of both surveys, the period and magnitude distributions obtained were significantly different, being longer and brighter in OGLE, and shorter and fainter in SuperMACHO, with ~ 500 δ Sct stars in common. Because SuperMACHO used a broad VR filter instead of V , we use these stars in common between the two catalogs in order to obtain the transformation

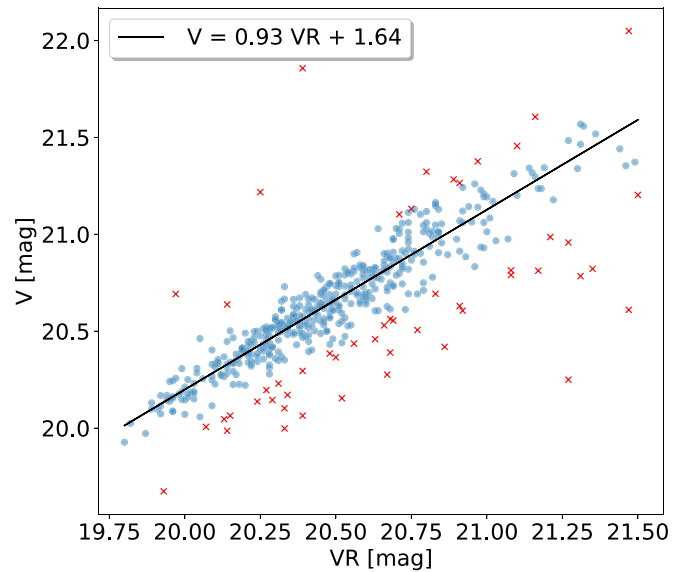


Figure 1. VR vs. V for the stars in common between OGLE and SuperMACHO. The black line shows the fit to the data. Only stars represented with blue filled circles have been used in the fit, while stars shown as open red crosses have been rejected by an iterative 2.5σ clipping algorithm.

to the V band. The transformation between VR and V did not show any color-term dependency for these stars. Figure 1 shows the graphic representation of the relation between VR (SuperMACHO) and V (OGLE). After applying a 2.5 sigma clipping over the V versus VR fit, we obtained the following relation:

$$V = 0.93 (\pm 0.01) \cdot VR + 1.6 (\pm 0.3). \quad (1)$$

The black line in Figure 1 is the fit to the data (blue circles) and the red crosses are those stars rejected from the σ clipping. The Pearson coefficient ($r = 0.95$) and the rms (0.09 mag) of this relation is also an indication that the transformation between these two bands for these stars follows a linear dependence and does not depend on other factors.

The top left panel of Figure 2 shows the PLR in M_V for the LMC δ Sct stars. In order to obtain a clean sample of δ Sct stars in the LMC, we remove those stars that are flagged with a remark in the Poleski et al. (2010) catalog. The vast majority of those removed (1488) are uncertain δ Sct stars, while 19 are Galactic δ Sct stars based on their proper motions and five with “variable mean luminosities.” On the other side, for the Garg et al. (2010) δ Sct star catalog we did not apply any restriction.

We detect an interesting feature to our knowledge never reported in previous studies; the PLR of the δ Sct in the LMC follows a broken power law rather than a single linear relation over the full period range ($-1.4 < \log P < -0.4$). Particularly, a segmented linear relation with a break-point at $\log P \simeq -1.03$ better reproduces this behavior (see Section 3.5).

It is worth noting that absolute V magnitudes were corrected after applying the proper A_V extinction to each individual star, using the LMC reddening map from Haschke et al. (2011). In addition, because of the extended structure of the LMC in the sky and its proximity, we correct the individual distances by the LMC geometry (van der Marel & Cioni 2001). Finally, we explored the influence of the depth of the LMC by generating random samples using the measured depths in the different parts of the LMC given by Subramanian & Subramanian (2009).

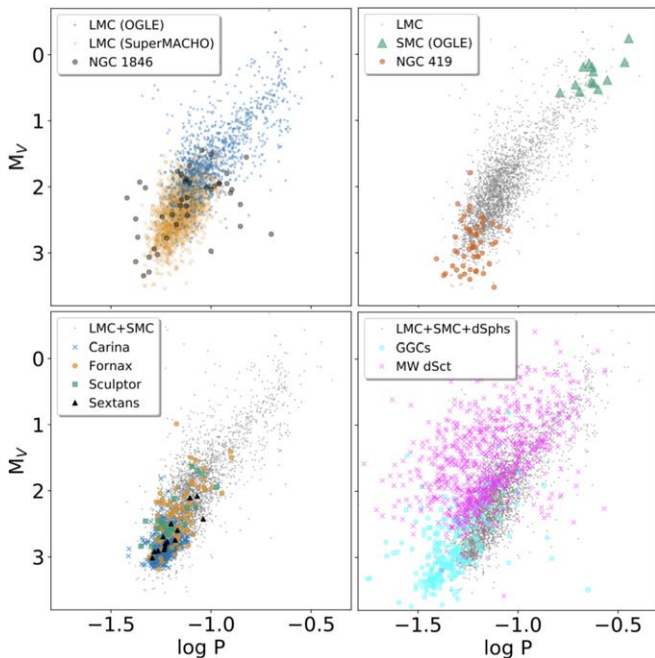


Figure 2. Period vs. absolute magnitude in V plane of δ Sct stars in different environments. Top left: the LMC. Top right: the SMC. For guidance, background gray dots represent the δ Sct stars from the LMC (combined OGLE + SuperMACHO sample). Bottom left: dSph galaxies. For guidance, background gray dots represent the δ Sct stars from the LMC and the SMC. Bottom right: Galactic (field and globular clusters) δ Sct stars. Background gray dots are the combined δ Sct samples from the LMC, the SMC, and dSph galaxies. See the main text for references for each sample.

We conclude that these effects are negligible, and that they are not causing a change of slope in the PLR. The top panel of Figure 2 includes the corrections by reddening and the LMC geometry.

Additionally, Salinas et al. (2018) found 55 δ Sct stars in a 5.5×5.5 area centered on the LMC globular cluster NGC 1846. Over 40 of them are outside two half-light radii, and probably belong to the LMC field. The δ Sct stars of Salinas et al. (2018) are represented by black circles in the top left panel of Figure 2.⁶ The majority of these stars are located around the bulk of the SuperMACHO sample, and except for a few outliers, i.e., around the region of shorter periods, follow a similar tendency.

3.2. SMC

The only search for δ Sct stars in the SMC before 2021 was done by OGLE. Soszynski et al. (2002) detected 19 candidates that they classified as “other variable stars” but they claimed that most of them are probably δ Sct stars. From this list, 17 have a period compatible with being δ Sct stars ($P \lesssim 0.3$ day).⁷ By visual inspection of the individual light curves, using periods reported by OGLE, two of them do not show a reliable light curve.⁸ Therefore, we end up with 15 stars detected by OGLE in the SMC as probable δ Sct stars.

In a recent work made by Martínez-Vázquez et al. (2021), we have detected 54 δ Sct stars in a field of 5.5×5.5 centered

on the SMC globular cluster NGC 419. A total of 48 δ Sct stars were two half-light radii outside of NGC 419, and therefore consistent with being δ Sct stars of the SMC field.

The top right panel of Figure 2 shows the PLR of the δ Sct stars detected in the field of the SMC so far. Green triangles are the 15 δ Sct stars detected by Soszynski et al. (2002), while the orange circles represent those δ Sct stars discovered by Martínez-Vázquez et al. (2021) in the field of the SMC globular cluster NGC 419. For clarity, a few δ Sct stars that seem to have aliased periods in the latter work were removed. As a guidance, we plot the LMC δ Sct stars that were displayed in the top left panel of Figure 2 as background gray dots. The difference between the period range (and luminosity) of both works is understandable given the nature of each study, and it reflects the need for obtaining a more complete study of δ Sct stars in the SMC. While the observation strategy of OGLE is better suited to detect variables like RR Lyrae stars and Cepheids that have timescales for variability > 0.5 day (rather than a few hours)—detecting therefore only the δ Sct stars with longer periods—the strategy of Martínez-Vázquez et al. (2021) was focused on the study of δ Sct stars. Besides, δ Sct stars were near the faint limit of OGLE and the most affected stars in terms of detection are the shorter period δ Sct stars since they are fainter. It is also worth noting that because of the time span of the observations of NGC 419, the δ Sct stars with periods larger than 0.2 days were difficult to detect in this study.

It is noticeable by looking at this panel how the larger and the shorter period δ Sct stars in the SMC follow the same tendency as in the LMC. This also supports the argument that the PLR of the δ Sct stars cannot be explained by only one linear relation but a segmented linear relation with a breakpoint at $\log P \simeq -1.03$.

3.3. Dwarf Spheroidal Galaxies

It was not until the past decade that δ Sct stars in dwarf galaxies started becoming relevant. Several factors played a fundamental role in this kind of study, the most important being deep photometry and high cadence. Mateo et al. (1998) discovered 20 δ Sct stars in Carina. More than 15 yr later, Vivas & Mateo (2013) reported the discovery of 340 δ Sct stars in Carina and Coppola et al. (2015) increased the sample of δ Sct stars in Carina in over 100 more. So far, Carina is the dwarf spheroidal (dSph) galaxy with the largest sample of δ Sct stars known; 426 δ Sct stars from the merger of the two previous works (Vivas et al. 2019). The second largest catalog in terms of δ Sct stars in dSph galaxies is Fornax with 85 δ Sct stars detected by Poretti et al. (2008), followed by Sculptor with 23 δ Sct (Martínez-Vázquez et al. 2016), and Sextans with 14 δ Sct stars (Vivas et al. 2019).

Carina and Fornax have extended star formation histories (see, e.g., Gallart et al. 2015) and therefore they will probably have a mixture of δ Sct stars coming from an old and metal-poor population (SX Phe) and δ Sct stars coming from a younger and more metal-rich population. In Sculptor and Sextans, on the other hand, all of their sample is composed by an old and metal-poor population, since both galaxies had an event of star formation more than 10 Gyr ago (de Boer et al. 2012; Bettinelli et al. 2018).

The bottom left panel of Figure 2 shows the period–luminosity (PL) plane of the δ Sct stars detected in each dSph. Again,

⁶ We excluded in this plot the δ Sct stars in NGC 1846 with probable aliased periods according to Salinas et al. (2018).

⁷ OGLE 004616.17-731416.1 and OGLE 005507.46-724434.0 have periods of 0.50 and 0.57 days, respectively.

⁸ OGLE 005008.48-725916.5 and OGLE 005259.56-725605.3

there is a good agreement with what we have seen in previous panels for the shorter periods of δ Sct stars.

3.4. Milky Way: Field Stars and Globular Clusters

Finally, we display in the bottom right panel of Figure 2 the Galactic δ Sct stars and the SX Phe that come from the GGCs. Interestingly, we can notice here a dual behavior that may be due to the different populations traced. While the GGCs harbor an old metal-poor population of δ Sct (SX Phe) stars, the Galactic field δ Sct stars are representatives of a metal-rich population. In fact, the fit that Ziaali et al. (2019) makes is in agreement with that from McNamara (2011) for $[\text{Fe}/\text{H}] = 0.0$ dex (see Section 3.6).

Another aspect to mention here is that the lower end of the global period–luminosity plane of δ Sct stars is ruled by the SX Phe from the GGCs, which do not follow the same relation as the Milky Way (MW) field δ Sct stars (see Fiorentino et al. 2015).

As mentioned in Section 2, we used the Galactic δ Sct sample as a comparison but we will not be using these data in the derivation of the PLR.

3.5. A Piecewise Linear Relation for the δ Sct's PLR

We compiled all the extragalactic data mentioned in the previous subsections and using an orthogonal distance regression (Boggs et al. 1988) we fit a piecewise linear relation to these data. To make the fit less sensitive to outliers, we used only those stars falling in regions of the period– M_V plane where the relative density of δ Sct stars is at least 10%. The slopes and the break-point of the piecewise linear relation are as follow:

$$\begin{aligned} M_V^{\text{sp}} &= -7.08(\pm 0.25)\log P - 5.74(\pm 0.29); \\ \log P &< -1.03 \end{aligned} \quad (2a)$$

$$\begin{aligned} M_V^{\text{lp}} &= M_V^{\text{sp}} + 4.38(\pm 0.32)(\log P + 1.03(\pm 0.01)); \\ \log P &\geq -1.03 \end{aligned} \quad (2b)$$

where sp and lp superscripts stand for shorter periods and longer periods than the break-point, respectively. The break-point derived is $\log P = -1.03 \pm 0.01$ ($P = 0.093 \pm 0.002$ days). The goodness of the fit given by the residual variance ($S_r^2 = 0.003$) indicates that this piecewise linear relation represents better these data than a single linear relation ($S_r^2 = 0.02$).

The newly derived PLR for extragalactic δ Sct stars is shown in the top left panel of Figure 3.

3.6. Comparison with Previous Relations

During the past few decades, there have been several efforts to obtain a PLR for the δ Sct stars. Some teams (Nemec et al. 1994 and Fiorentino et al. 2015) derived relations for different δ Sct pulsators (especially for fundamental, F, and first overtone, FO), but others (McNamara 2011) obtained the PLR for only F δ Sct. In practice, it is very difficult to distinguish different pulsation modes from an observational point of view (see, e.g., Soszynski et al. 2002). This is the reason why we did not make any distinction in Section 3.5 when obtaining our PLR (Equations (2b) and (2a)). Moreover, OGLE and SuperMACHO first overtone and double-mode pulsators, when present, occupy basically the same position in the period– M_V plane than the fundamental pulsators.

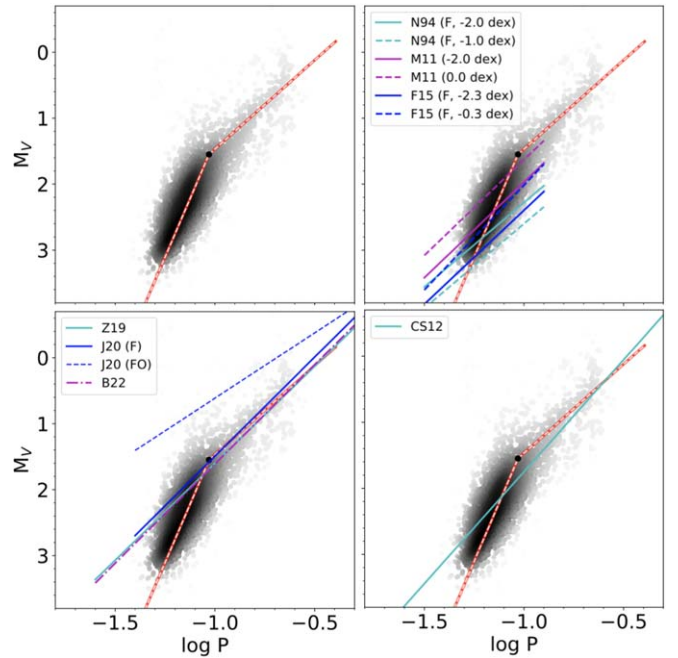


Figure 3. Density map of the δ Sct stars in the period vs. absolute magnitude in V plane. The top left panel shows the fit obtained in this work while the rest of the panels show a comparison between this new fit and previous PLR available in the literature. References: N94 (Nemec et al. 1994), M11 (McNamara 2011), CS12 (Cohen & Sarajedini 2012), F15 (Fiorentino et al. 2015), Z19 (Ziaali et al. 2019), J20 (Jayasinghe et al. 2020).

Figure 3 shows a comparison between our derived PLR and previously obtained relations. Particularly, the top right panel displays the PL obtained by Nemec et al. (1994), McNamara (2011), and Fiorentino et al. (2015). The pioneering work of Nemec et al. (1994) assessed a PLR using 21 (15 F and 6 FO) δ Sct (or SX Phe) stars from GGCs, while McNamara (2011) used 20 δ Sct stars of the field of the Milky Way. On the other hand, the Fiorentino et al. (2015) relationships shown here are purely theoretical, obtained from pulsation models for main-sequence stars computed assuming $Z = 0.0001$ and $Z = 0.008$ (i.e., $[\text{Fe}/\text{H}] = -2.3$ and -0.3 , since they consider α -enhanced stellar evolution models).

The bottom left panel of Figure 3 shows the comparison with the recently derived PLR for the Galactic δ Sct stars using different data sets. Ziaali et al. (2019) is based on 228 stars from the Rodríguez et al. (2000) catalog plus 1124 stars observed by the Kepler mission, while the Jayasinghe et al. (2020) catalog used the all-sky catalog of ~ 8400 δ Sct stars in ASAS-SN, both using distances from Gaia DR2. The Ziaali et al. (2019) relation is very similar to the McNamara (2011) relation but the former was extended in the longer period range that is seen only in the Galactic and Magellanic Clouds δ Sct stars. Both relations are similar (despite an offset in the zero-point) and agree with the long-period end of the piecewise PLR obtained in this work. More recently, Barac et al. (2022) revised Ziaali et al. (2019) PLR using Gaia DR3 parallaxes also obtaining similar results.

The bottom right panel of Figure 3 presents the comparison with the relation obtained by Cohen & Sarajedini (2012), who made a fit over the entire period range of δ Sct stars (including the SX Phe coming from the GGCs). There is a clear discrepancy between both relations. However, the Cohen & Sarajedini (2012) relation was obtained using only some of the Poleski et al. (2010) δ Sct stars in the LMC, the very few δ Sct stars that were known in Carina (Mateo et al. 1998), and none from Sculptor and

Sextans, Fornax (Poretti et al. 2008) being the most significant one in terms of δ Sct stars at that time. The inclusion of stars discovered after 2012 in the dSph galaxies mentioned (Carina: Vivas & Mateo 2013; Coppola et al. 2015, Sculptor: Martínez-Vázquez et al. 2016, Sextans: Vivas et al. 2019), plus the LMC δ Sct stars detected by Garg et al. (2010), in the period– M_V plane opens a new debate about the origin of the PLR in the δ Sct stars since it is clearly noticeable that a new behavior is governing the shorter period range.

3.7. Possible Causes

In the following we will review the main causes that could explain this behavior in the PLR of the δ Sct stars.

1. *Metallicity effect.* The fact that the break in the PLR of the δ Sct stars comes from the metallicity is unlikely. The strongest argument that supports this is that the main contributions to Figure 3 come from Poleski et al. (2010) and Garg et al. (2010), and both samples cover the same regions of the LMC. However, they obey different relations. While the Poleski et al. (2010) sample represents a larger period range and follows Equation (2b), the Garg et al. (2010) sample fills the lower period end and follows better Equation (2a). The existence of any metallicity gradients should be present in both samples (i.e., for longer and shorter periods), and not be reflected in only one of them. In addition, bearing in mind that the metallicity of the LMC is between $[\text{Fe}/\text{H}] = -0.3$ and -0.7 dex (Grocholski et al. 2006; Carrera et al. 2008b), there are no PLRs that can explain, with these metallicities, the large luminosity dispersion observed in the short period range (see Figure 3). Although we do not discard the fact that there may be metallicity dependence in the PL, we point out that this would not be the main driver that is causing this in the PLR of the δ Sct stars.

Moreover, by looking at Figure 2 (especially the bottom left panel) we see that the inclusion of several systems with different metallicities (see Table 1) does not produce any clear trend in the period– M_V plane predicted by the metallicity of previously derived relations (see Section 3.6, top right panel of Figure 2). Those systems seem to follow the same relation.

2. *Depth and geometry effects.* This effect was shown to be almost negligible in the LMC (see Section 3.1) and it would be less significant for farther galaxies.
3. *Pulsation mode.* We also investigated the possible association of this broken relation as due to the pulsation mode of the δ Sct stars. The different pulsators (fundamental, first overtone, multimode) in the Poleski et al. (2010) and Garg et al. (2010) samples did not shed any light on this hypothesis. First overtone and multimode pulsators are *brighter* than fundamental pulsators (see, e.g., Jayasinghe et al. 2020); therefore they cannot be the reason of the behavior seen at fainter and shorter periods. Thus, we also discarded the pulsation mode as a possible origin of the broken PLR relation.

We speculate that a segmented PLR may be naturally present in sufficiently metal-poor systems (i.e., with LMC-like metallicities or lower), and that an attempt to reproduce this behavior should be made using state-of-the-art stellar pulsation and evolution models, coupled with synthetic populations tools that

properly mimic the properties of δ Sct and SX Phe stars in the metal-poor systems studied in this Letter.

A similar behavior (although less pronounced) has been observed in the PLR of Cepheids of the LMC (e.g., Bhardwaj 2020). They could not explain either the physics behind it. The broken power-law relation seen in the δ Sct stars is evident in the data collected from the extragalactic sources and future investigations will provide more knowledge about the physics behind this particular behavior.

4. Final Remarks

In this Letter, we have used 3664 δ Sct stars from eight different extragalactic stellar systems. Such a large sample, spanning all period ranges for these types of stars, has revealed a broken PLR not seen before in the MW δ Sct stars. In particular, we statistically tested that the best representation of the extragalactic δ Sct stars is by a piecewise linear relation of the form given by Equations (2a) and (2b).

We have shown that this new dependence is not due to depth or geometric effects in the extragalactic sources as they proved to be negligible. Also, it most likely not caused by metallicity effects, since both SuperMACHO and OGLE studied the same region of the LMC, therefore probing the same metallicity range. Furthermore, the pulsation mode of the δ Sct stars seems not to be causing this effect either. The origin of the segmented relation at ~ 0.09 days remains still unknown based on the current data. A new survey focused on short period variables, delivering a homogeneous sample of δ Sct, would either confirm or reject the new PLR proposed here.



C.E.M.-V. would like to dedicate this Letter to the memory of her late father. C.E.M.-V. also thanks Elham Ziaali for providing the catalog of Galactic δ Sct stars and John Blakeslee for useful conversations and advice. We are also grateful to the anonymous referee for helpful suggestions.

C.E.M.-V. and R.S. are supported by the international Gemini Observatory, a program of NSF’s NOIRLab, which is managed by the Association of Universities for Research in Astronomy (AURA) under a cooperative agreement with the National Science Foundation, on behalf of the Gemini partnership of Argentina, Brazil, Canada, Chile, the Republic of Korea, and the United States of America.

Software: SciPy (Virtanen et al. 2020), Astropy (Astropy Collaboration et al. 2013), NumPy, (Harris et al. 2020), Pandas (McKinney et al. 2010), Matplotlib (Hunter 2007), TOPCAT (Taylor 2005)

Note added in proof. During the publication of this Letter, V. Ripepi kindly pointed out to us that a nonlinear PLR for Galactic δ Sct stars has recently been independently reported by Gaia Collaboration et al. (2022), based on data from Gaia DR3.

ORCID iDs

C. E. Martínez-Vázquez  <https://orcid.org/0000-0002-9144-7726>
 R. Salinas  <https://orcid.org/0000-0002-1206-1930>
 A. K. Vivas  <https://orcid.org/0000-0003-4341-6172>
 M. Catelan  <https://orcid.org/0000-0001-6003-8877>

References

- Astropy Collaboration, Robitaille, T. P., Tollerud, E. J., et al. 2013, *A&A*, 558, A33
 Barac, N., Bedding, T. R., Murphy, S. J., & Hey, D. R. 2022, *MNRAS*, 516, 2080

- Baumgardt, H., & Hilker, M. 2018, *MNRAS*, **478**, 1520
- Bettinelli, M., Hidalgo, S. L., Cassisi, S., Aparicio, A., & Piotto, G. 2018, *MNRAS*, **476**, 71
- Bhardwaj, A. 2020, *JApA*, **41**, 23
- Boggs, P. T., Spiegelman, C. H., Donaldson, J. R., & Schnabel, R. B. 1988, *J. Econom.*, **38**, 169
- Braga, V. F., Dall’Ora, M., Bono, G., et al. 2015, *ApJ*, **799**, 165
- Braga, V. F., Stetson, P. B., Bono, G., et al. 2018, *AJ*, **155**, 137
- Carrera, R., Gallart, C., Aparicio, A., et al. 2008a, *AJ*, **136**, 1039
- Carrera, R., Gallart, C., Hardy, E., Aparicio, A., & Zinn, R. 2008b, *AJ*, **135**, 836
- Carretta, E., Bragaglia, A., Gratton, R., D’Orazi, V., & Lucatello, S. 2009, *A&A*, **508**, 695
- Catelan, M., Pritzl, B. J., & Smith, H. A. 2004, *ApJS*, **154**, 633
- Catelan, M., & Smith, H. A. 2015, *Pulsating Stars* (New York: Wiley)
- Cohen, R. E., & Sarajedini, A. 2012, *MNRAS*, **419**, 342
- Coppola, G., Marconi, M., Stetson, P. B., et al. 2015, *ApJ*, **814**, 71
- de Boer, T. J. L., Tolstoy, E., Hill, V., et al. 2012, *A&A*, **539**, A103
- Dekany, I., Minniti, D., Catelan, M., et al. 2013, *ApJL*, **776**, L19
- Fiorrentino, G., Marconi, M., Bono, G., et al. 2015, *ApJ*, **810**, 15
- Gaia Collaboration, Brown, A. G. A., Vallenari, A., et al. 2018, *A&A*, **616**, A1
- Gaia Collaboration, De Ridder, J., Ripepi, V., et al. 2022, arXiv:2206.06075
- Gallart, C., Monelli, M., Mayer, L., et al. 2015, *ApJL*, **811**, L18
- Garg, A., Cook, K. H., Nikolaev, S., et al. 2010, *AJ*, **140**, 328
- Goudfrooij, P., Girardi, L., Kozhurina-Platais, V., et al. 2014, *ApJ*, **797**, 35
- Goudfrooij, P., Puzia, T. H., Kozhurina-Platais, V., & Chandar, R. 2009, *AJ*, **137**, 4988
- Graczyk, D., Pietrzyński, G., Thompson, I. B., et al. 2014, *ApJ*, **780**, 59
- Grocholski, A. J., Cole, A. A., Sarajedini, A., Geisler, D., & Smith, V. V. 2006, *AJ*, **132**, 1630
- Harris, W. E. 1996, *AJ*, **112**, 1487
- Harris, C. R., Millman, K. J., van der Walt, S. J., et al. 2020, *Natur*, **585**, 7825
- Haschke, R., Grebel, E. K., & Duffau, S. 2011, *AJ*, **141**, 158
- Hubble, E. 1929, *PNAAS*, **15**, 168
- Hubble, E. P. 1925, *Obs*, **48**, 139
- Hunter, J. D. 2007, *CSE*, **9**, 90
- Jayasinghe, T., Stanek, K. Z., Kochanek, C. S., et al. 2020, *MNRAS*, **493**, 4186
- Kirby, E. N., Cohen, J. G., Guhathakurta, P., et al. 2013, *ApJ*, **779**, 102
- Kirby, E. N., Lanfranchi, G. A., Simon, J. D., Cohen, J. G., & Guhathakurta, P. 2011, *ApJ*, **727**, 78
- Koch, A., Grebel, E. K., Wyse, R. F. G., et al. 2006, *AJ*, **131**, 895
- Leavitt, H. S., & Pickering, E. C. 1912, *HarCi*, **173**, 1
- Martínez-Vázquez, C. E., Salinas, R., & Vivas, A. K. 2021, *AJ*, **161**, 120
- Martínez-Vázquez, C. E., Monelli, M., Bono, G., et al. 2015, *MNRAS*, **454**, 1509
- Martínez-Vázquez, C. E., Monelli, M., Bernard, E. J., et al. 2017, *ApJ*, **850**, 137
- Martínez-Vázquez, C. E., Stetson, P. B., Monelli, M., et al. 2016, *MNRAS*, **462**, 4349
- Martínez-Vázquez, C. E., Vivas, A. K., Gurevich, M., et al. 2019, *MNRAS*, **490**, 2183
- Mateo, M., Hurley-Keller, D., & Nemeč, J. 1998, *AJ*, **115**, 1856
- Mateo, M., Olszewski, E. W., Pryor, C., Welch, D. L., & Fischer, P. 1993, *AJ*, **105**, 510
- McKinney, W., et al. 2010, in Proc. of the 9th Python in Science Conf., ed. S. van der Walt & J. Millman, **56**, <https://conference.scipy.org/proceedings/scipy2010/mckinney.html>
- McNamara, D. H. 2011, *AJ*, **142**, 110
- Mucciarelli, A. 2014, *AN*, **335**, 79
- Murphy, S. J., Hey, D., Van?Reeth, T., & Bedding, T. R. 2019, *MNRAS*, **485**, 2380
- Neeley, J. R., Marengo, M., Bono, G., et al. 2015, *ApJ*, **808**, 11
- Nemeč, J. M., Nemeč, A. F. L., & Lutz, T. E. 1994, *AJ*, **108**, 222
- Pietrzyński, G., Graczyk, D., Gallenne, A., et al. 2019, *Natur*, **567**, 200
- Poleski, R., Soszyński, I., Udalski, A., et al. 2010, *AcA*, **60**, 179
- Poretti, E., Clementini, G., Held, E. V., et al. 2008, *ApJ*, **685**, 947
- Riess, A. G., Casertano, S., Yuan, W., Macri, L. M., & Scolnic, D. 2019, *ApJ*, **876**, 85
- Rizzi, L., Held, E. V., Saviane, I., Tully, R. B., & Gullieuszik, M. 2007, *MNRAS*, **380**, 1255
- Rodríguez, E., López-González, M. J., & López de Coca, P. 2000, *A&AS*, **144**, 469
- Salinas, R., Pajkos, M. A., Vivas, A. K., Strader, J., & Contreras Ramos, R. 2018, *AJ*, **155**, 183
- Soszyński, I., Udalski, A., Szymanski, M., et al. 2002, *AcA*, **52**, 369
- Subramanian, S., & Subramanian, A. 2009, *A&A*, **496**, 399
- Taylor, M. B. 2005, in ASP Conf. Ser. 347, *Astronomical Data Analysis Software and Systems XIV*, ed. P. Shopbell, M. Britton, & R. Ebert (San Francisco, CA: ASP), **29**
- van der Marel, R. P., & Cioni, M. -R. -L. 2001, *AJ*, **122**, 1807
- Virtanen, P., Gommers, R., Oliphant, T. E., et al. 2020, *NatMe*, **17**, 261
- Vivas, A. K., Alonso-García, J., Mateo, M., Walker, A., & Howard, B. 2019, *AJ*, **157**, 35
- Vivas, A. K., Martínez-Vázquez, C. E., Walker, A. R., et al. 2022, *ApJ*, **926**, 78
- Vivas, A. K., & Mateo, M. 2013, *AJ*, **146**, 141
- Vivas, A. K., Olsen, K., Blum, R., et al. 2016, *AJ*, **151**, 118
- Westerlund, B. E. 1997, *The Magellanic Clouds* (Cambridge: Cambridge Univ. Press)
- Ziaali, E., Bedding, T. R., Murphy, S. J., Van?Reeth, T., & Hey, D. R. 2019, *MNRAS*, **486**, 4348